CRISPR-based Colorimetric Nucleic Acid Tests for Visual Readout of DNA Barcode for Food Authenticity

Xinying Yin[1], Hao Yang[2], Yongzhe Piao[1], Yulin Zhu[2], Qiuyue Zheng[1], Mohammad Rizwan Khan[3], Yong Zhang[2], Rosa Busquets[4], Bing Hu[1], Ruijie Deng[2,*], Jijuan Cao[1,*]

[1] Key Laboratory of Biotechnology and Bioresources Utilization of Ministry of Education, Dalian Minzu University, Dalian 116600, China

[2] College of Biomass Science and Engineering, Healthy Food Evaluation Research Center, Sichuan University, Chengdu 610065, China

[3] Department of Chemistry, College of Science, King Saud University, Riyadh, 11451, Saudi Arabia

[4] School of Life Sciences, Pharmacy and Chemistry, Kingston University, Penrhyn Road, KT1 2EE, Kingston Upon Thames, United Kingdom

* Corresponding authors: drj17@scu.edu.cn; caojijuan@dlnu.edu.cn

Abstract

Food authenticity is a critical issue associated with the economy, religion, and food safety. Herein, we report a label-free and colorimetric nucleic acid assay for detecting DNA barcodes, enabling the determination of food authenticity with the naked eye. This method, termed the CRISPR-based colorimetric DNA barcoding (Cricba) assay, utilizes CRISPR/Cas12a (CRISPR = clustered regularly interspaced short palindromic repeats; Cas = CRISPR associated protein) to specifically recognize the polymerase chain reaction (PCR) products for further *trans*-cleavaging the peroxidase-mimicking G-quadruplex DNAzyme. Based on this principle, the presence of the cytochrome oxidase subunit I gene could be directly observed with the naked eye via the color change of 3,3′,5,5′-tetramethylbenzidine sulfate (TMB). The whole detection process, including PCR amplification and TMB colorimetric analysis, can be completed within 90 min. The proposed assay can detect pufferfish concentrations diluted to 0.1% (w/w) in a raw pufferfish mixture, making it one of the most sensitive methods for food authenticity. The robustness of the assay was verified by testing four common species of pufferfish, including *Lagocephalus inermis*, *Lagocephalus spadiceus*, *Takifugu bimaculatus*, and *Takifugu alboplumbeus*. The assay is advantageous in easy signal readout, high sensitivity, and general applicability and thus could be a competitive candidate for food authenticity.

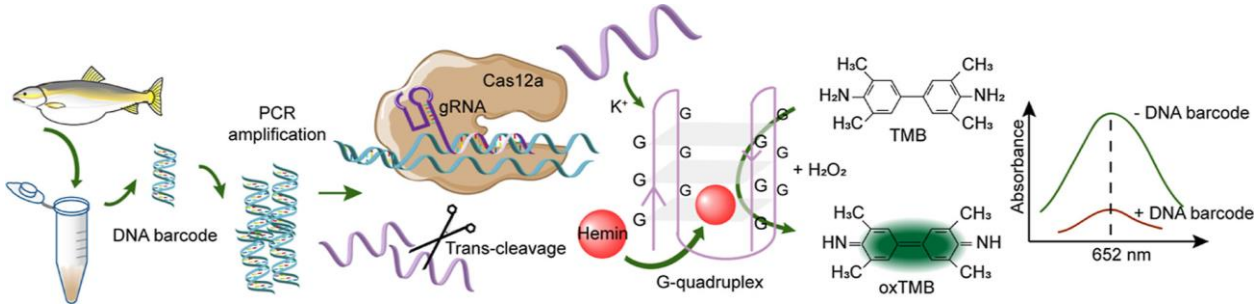

Scheme 1. Schematic Illustration of the Cricba Assay for Visual Detection of DNA Barcode and Food Authenticity

Keywords: food authenticity CRISPR-cas DNA barcode pufferfish COI gene

Introduction

Food authenticity represents an economic and potential food safety problem for industry, consumers, and governments worldwide. (1) The main food authenticity issue practices met in the meat industry sector are substitutions of meat ingredients with other animal species, breeds, tissues, and proteins, and will ultimately have an adverse impact on food safety and the confidence of the consumer. (2) Seafood products are especially susceptible to food authenticity issues, especially with respect to ultimate species substitution and mislabeling. (3) Pufferfish (Tetraodontidae) have long been considered toxic to humans as they contain a heat-stable and water-soluble neurotoxin called tetrodotoxin (TTX), which is over 1000 times more toxic to humans than cyanide and has no known antidote. (4,5) In spite of this, some pufferfish species are still traditional delicacies in Asian countries. (6) In China, the pufferfish species *Takifugu rubripes* and T. obscurus are allowed to be cultured by specific companies and sold after processing. (7,8) However, when a complex manufacturing process is involved, or in the case of fish being sold as parts, classical identification methods based on distinctive morphological features are ineffective. (9) Thus, consumers may still face the risk of TTX poisoning due to the trade of products with wrong labels being illegally sold on the domestic market. In order to guarantee consumers' safety, the authenticity of pufferfish products that are imported and purchased goods must be checked.

Protein-based detection methods, such as the enzyme-linked immunosorbent assay (10) and immunosensors, (11) have been developed for food authenticity. However, high temperatures and other conditions will lead to the denaturation of target proteins. Therefore, protein-targeted tools could hardly be used for the authenticity of processed foods. (12) Nucleic acid-based methods can recognize any life form with specificity, and DNA can endure high temperatures and remain stable, so that it can be used as a specific and stable biomarker for the authenticity of both unprocessed and processed food. (13) DNA barcoding is a new identification method which allows species identification, utilizing a short sequence of DNA from high-interspecific and low-intraspecific variability. (9,14) For example,

the cytochrome xxidase sub-unit I (COI) gene as a DNA barcode has been widely applied in various branches of biological sciences, including forensic genetics, (15) biodiversity, (16) and seafood identification. (17,18) Traditionally, PCR-based methods and real-time quantitative PCR (qPCR)-based methods are very sensitive for food authenticity detection. (19,20) Subsequently, isothermal amplification techniques, such as loop-mediated isothermal amplification and recombinase polymerase amplification, enable nucleic acid amplification at a constant temperature and have a high amplification efficiency. (21,22) Polymerase chain reaction (PCR) dominates in the identification of food species by targeting DNA barcodes due to its mature technology and readily available reagents and kits. (23,24) However, the potential issue caused by these methods is the risk of non-specific amplification. Methods to ease the signal readout and alleviate non-specific amplification would increase the applicability and robustness of PCR for food authenticity. (25)

CRISPR/Cas12a (clustered regularly interspaced short palindromic repeats and CRISPR-associated protein) exhibits non-specific cleavage activity against single-stranded (ss) DNA and has been used to convert sequence-specific information into fluorescent, electrochemical, and chromogenic signals. (26−31) The CRISPR system can recognize and target invasive nucleic acids by utilizing CRISPR RNAs (crRNAs, also named gRNA) as guide molecules. Based on this principle, CRISPR-Cas12a has been developed for the detection of amplicons produced by PCR or isothermal amplification. (32−35) The combination of nucleic acid amplification and the CRISPR-Cas system has greatly increased the specificity and sensitivity for detecting target RNA/DNA, and these assays have been applied to detect pathogens and nucleic acid biomarkers. (36−38)

Here, we introduced CRISPR into the PCR method to create a nucleic acid colorimetric assay for visual readout of DNA barcodes, allowing highly sensitive and reliable food authenticity via the naked eye. The proposed CRISPR-based colorimetric DNA barcoding (Cricba) assay combined the catalytic activity of DNAzyme, the high amplification efficiency of PCR, and the specificity of the CRISPR/Cas12a system to identify species-specific DNA barcodes, thus improving the practicality of

food authentication. We applied the Cricba assay to verify four pufferfish species' DNA barcodes for the cytochrome oxidase subunit I (COI) gene. The Cricba assay permitted us to identify the pufferfish species and content in mixed meat. The CRISPR-based colorimetric nucleic acid tests are promising in food authentication and thereby would broaden the application of the CRISPR-Cas system in food quality analysis.

Materials and Methods

Materials and Reagents

Oligonucleotide sequences were synthesized by Sangon Biotech (Shanghai, China) (Table S1, in the Supporting Information). All synthesized DNA sequences were purified by PAGE. LbCas12a was purchased from Tolobio (Shanghai, China). 2 × Easy PCR SuperMix was purchased from Transgen (Beijing, China). Platinum SYBR Green qPCR SuperMix-UDG w/ROX and phi29 DNA polymerase (20 U/μL) were bought from Thermo Fisher Scientific (Waltham, USA). The dNTP solution mix, rNTP solution mix, DNase I (2000 U/mL), and T7 RNA polymerase (20 U/μL) were acquired from New England Biolab (Ipswich, MA, USA). Agarose, 50 × TAE buffer, 10,000 × GelRed dye, and 6 × loading buffer were purchased from Beijing DingGuo Biotech (Beijing, China). Soluble TMB substrate solution and TIANamp genomic DNA kits were bought from Tiangen (Beijing, China). All the reagents were melted by molecular biology grade H2O (Corning, New York, USA). The sequences of the pufferfish cytochrome oxidase subunit I gene (COI gene) were obtained from NCBI.

Sample Preparation and DNA Extraction

All pufferfish samples were provided by the Fisheries Research Institute of Fujian, including *Lagocephalus inermis* (GenBank: KT833769), *T. fasciatus* (GenBank: KT833771), *L. spadiceus* (GenBank: KT833773), *T. rubripes* (GenBank: KT833774), *L. gloveri* (GenBank: KT833775), *T. bimaculatus* (GenBank: KT833778), *T. oblongus* (GenBank: KT833777), and *T. alboplumbeus* (GenBank: KT833780). All of the pufferfish samples were cut into pieces, ground in a mortar by

adding liquid nitrogen until the samples were ground into a powder, and then stored at −20 °C. In each reaction, 50 mg of raw pufferfish meat powder was used to extract DNA. Different pufferfish species' genomic DNA was extracted through the TIANamp genomic DNA kit according to the instructions. The extracted DNA concentration was determined through the absorbance value at 260 nm measured by the Microplate Reader Synergy H1 (BioTek, USA).

gRNA Preparation

gRNAs were obtained through in vitro transcription. The transcription reaction volume was 40 μL, with the template gRNA (100 μM) volume, 0.3 μL; T7 promoter (100 μM), 0.3 μL; 10 × phi29 buffer, 3 μL; and H_2O, 27.1 μL. The mixture was incubated at 90 °C for 3 min and at 25 °C for 30 min. Then, 1 μL of dNTP mix (10 mM each for dATP, dTTP, dCTP, and dGTP) and 0.3 μL (20 U/μL) of phi29 DNA polymerase were added into the mixture and incubated at 30 °C for 30 min and then inactivated at 65 °C for 10 min. Then, 2 μLof rNTP mix (25 mM each for rATP, rUTP, rCTPt, and rGTP), 2 μL of T7 RNA polymerase (20 U/μL), and 4 μL of 10 × T7 RNA polymerase buffer were added and incubated at 37 °C overnight. Then, the transcription products of gRNA were obtained. Finally, 4 μL of DNase I (2000 U/mL) was added to eliminate the residual DNA template, reacting at 37 °C for 2 h. Then, DNase I was inactivated by reaction at 65 °C for 10 min.

CRISPR/Cas12a Assay for Detecting Pufferfish DNA Barcodes

PCR amplification was performed in 20 μL volume, including the forward primer (10 μM), 1 μL; reverse primer (10 μM), 1 μL; 2 × Easy PCR SuperMix, 10 μL; extracted DNA (10 ng/μL), 1 μL; and H_2O, 7 μL, and then the above mixture was reacted through the ProFlex PCR System (ABI, USA). It was carried out based on the temperature program: 95 °C for 5 min and then 25 cycles of 95 °C for 15 s, 55 °C for 15 s, 72 °C for 45 s, and finally 72 °C for 7 min. Then, the detection based on the CRISPR-Cas12a system was carried out in a volume of 40 μL containing 4 μL of 10 × TOLO buffer 3, 0.4 μL

of LbCas12a protein (10 μM), 4 μL of transcription gRNA (2 μM), and 29.6 μL of H_2O incubated at 37 °C for 10 min. Finally, 1 μL of PCR product and 1 μL of G-quadruplex (10 μM) were added and reacted at 37 °C for 1 h. Reactions were stopped by heating at 65 °C for 10 min.

G-Quadruplex DNAzyme-Assisted Colorimetric Reaction

The 100 μL reaction system, which contained 40 μL of CRISPR-Cas12a reaction system, 5 μL of hemin (10 μM), 2 μL of KCl (1 M), 3 μL of H2O, and 50 μL of soluble TMB substrate solution (containing H2O2) was reacted at room temperature for 20 min, and then the result was observed with the naked eye. The absorbance of the reaction solution was measured by the microplate reader Synergy H1 (BioTek, USA). The *trans*-cleavage of G-quadruplex by Cas12a protein was verified using polyacrylamide gel electrophoresis (15%), and the gel images were obtained by the Champ Gel 7000 system (Sage Creation, Beijing, China).

qPCR-Based Detection of Pufferfish DNA Barcodes

Real-time PCR was performed by the CFX 96 Real-Time System (Bio-Rad, USA). The real-time PCR mixture was 20 μL, which contained 0.4 μL of forward primer (10 μM), 0.4 μL of reverse primer (10 μM), 10 μL of Platinum SYBR Green qPCR SuperMix, 8.2 μL of H2O, and 1 μL of extracted DNA (10 ng/μL). It was carried out based on the temperature program: initial denaturation at 95 °C for 10 min, followed by 40 cycles at 95 °C for 10 s, 60 °C for 30 s, and fluorescence acquisition was performed at each cycle.

Results and Discussion

Working Principle of the Cricba Assay

To establish a specific, sensitive, and visual DNA barcode assay for pufferfish species analysis, we integrated PCR amplification and the CRISPR-Cas12 *trans*-cleavage DNAzyme process (Figure 1 and

Scheme 1). DNA samples were extracted from pufferfish samples. The employed PCR amplified the specific DNA barcode of pufferfish, therein, the DNA region at the pufferfish COI gene was selected, followed by the CRISPR-Cas12a system to identify the PCR amplicon. In this assay, the applied gRNA was designed to specifically identify the PCR amplicon to eliminate non-specific amplification. The PCR amplicon worked as an activator to activate the *trans*-cleavage activity of the Cas12a enzyme, allowing it to cleave the single-stranded DNA G-quadruplex and prevent the formation of the G-quadruplex structure, which further inhibits the peroxidase-like activity and cannot catalyze the color development of TMB. In contrast, in the absence of the DNA barcode amplification products, the CRISPR-Cas12a/gRNA complex could not cleave the G-quadruplex. The intact G-quadruplex can bind hemin and catalyze the TMB that turned green (Figure 1A). In this way, the results can be easily distinguished via color differences between positive and negative samples. Sequentially, DNA barcodes were identified by both PCR primers and the CRISPR-Cas12a system, enabling a specific identification of pufferfish species.

Figure 1. Validation of the working principle of the Cricba assay. Absorbance analysis of the PCR amplification (A) and the Cas12a *trans*-cleavage G-quadruplex process (B) activated by the target DNA barcode. Electrophoresis analysis for the PCR amplification (C) and the target DNA-activation of Cas12a *trans*-cleavage G-quadruplex process (D). (E) Products and their structures corresponding to each electrophoretic band in (C) and (D).

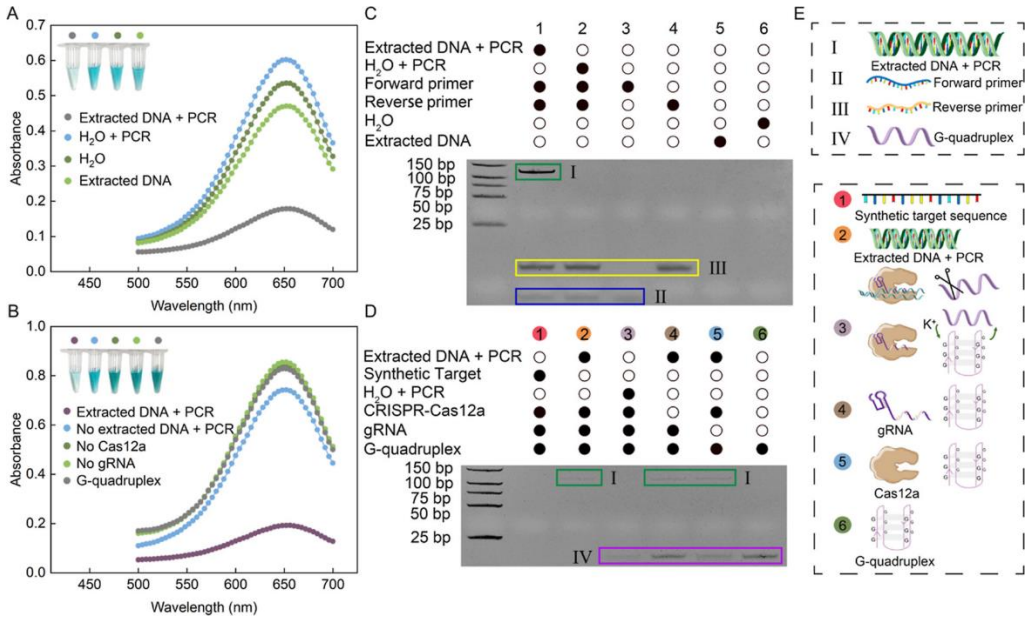

The working principle of CRISPR-Cas12a/gRNA *trans*-cleavage G-quadruplex was investigated via the absorbance of the reaction solution. The presence of the target PCR amplicon dramatically decreased the absorbance of TMB. The absence of Cas12a protein, gRNA, or target PCR amplicon, however, led to weak absorbance reduction (labeled "No Cas12a," "No gRNA," and "No target," respectively) (Figure 1B). This result manifested that the lack of Cas12a protein, gRNA, or target could not activate cleavage activity. While with the addition of 10 ng of extracted pufferfish DNAs (labeled "Extracted Target DNA"), the absorbance decreased from 0.664 to 0.537, compared to the system without added pufferfish DNA (Figure 1B). Meanwhile, the presence of PCR amplification products of the pufferfish COI gene on the above basis (labeled "Target PCR amplicon") resulted in a dramatic decrease in absorbance (0.743 to 0.193) compared to that in the absence of pufferfish DNA (labeled "H2O PCR amplicon"), which resulted in a signal-to-background difference (Δ A) of 0.576. The electrophoretic image also indicated that when the Cas12a protein, gRNA, and target DNA were present, the *trans*-cleavage activity of Cas12a protein could be activated (Figure 1B). The results indicated that the involvement of the PCR method can activate the cleavage of CRISPR-Cas12a.

Therefore, identification of pufferfish contamination in food samples could be identified by monitoring the absorbance change in the reaction solution.

gRNA Screening

Due to the complex secondary structure of genes and the sequence preference of the CRISPR-Cas system, the selection of gRNA is the most crucial factor for the detection performance of the CRISPR-Cas12 system. Accordingly, we chose 24 gRNA target binding sites (highlighted in blue) and protospacer adjacent motif (PAM) sites (highlighted in red) to identify four different species of pufferfish, including *L. inermis* (tested 8 gRNAs), *L. spadiceus* (tested 6 gRNAs), *T. bimaculatus* (tested 5 gRNAs), and *T. alboplumbeus* (tested 5 gRNAs). All gRNAs were designed according to the region on the COI gene (Figure S2, in the Supporting Information). For *L. inermis*, 8 gRNAs satisfied the requirement of PAM sequences (Figure 2A). The gRNAs were screened to exclude potential non-specific binding sites of other pufferfish species in COI genes using the online Blast alignment tool in the NCBI database (http://www.ncbi.nlm.nih.gov/blast). For L. inermis, gRNA8 achieved the highest specificity (Figure 2B), and the absorbance change ΔA, in the presence of extracted DNA at 652 nm was up to 0.651. Meanwhile, gRNA8 maintained high specificity to exclude the response to other pufferfish species. Species-specific gRNAs were also screened with respect to the other three species of pufferfish containing *L. spadiceus, T. bimaculatus,* and *T. alboplumbeus* (Figure S3, in the Supporting Information). The result showed that the assay could distinguish closely related species. The high specificity was contributed by the dual recognition based on PCR primers and gRNA.

Figure 2. Figure 2. Investigation of the gRNA locus on the capacity to discriminate different pufferfish species. (A) Sites of the PCR primer and gRNA targeting COI gene of L. inermis. (B) ΔA using gRNA in (A) response to different pufferfish species. The cytochrome oxidase subunit I (COI) genes' GenBank number of eight pufferfish species are shown in (B). ΔA indicates the difference in absorbance at 652 nm in the presence of L. inermis COI gene DNA to that in the absence of L. inermis COI gene DNA.

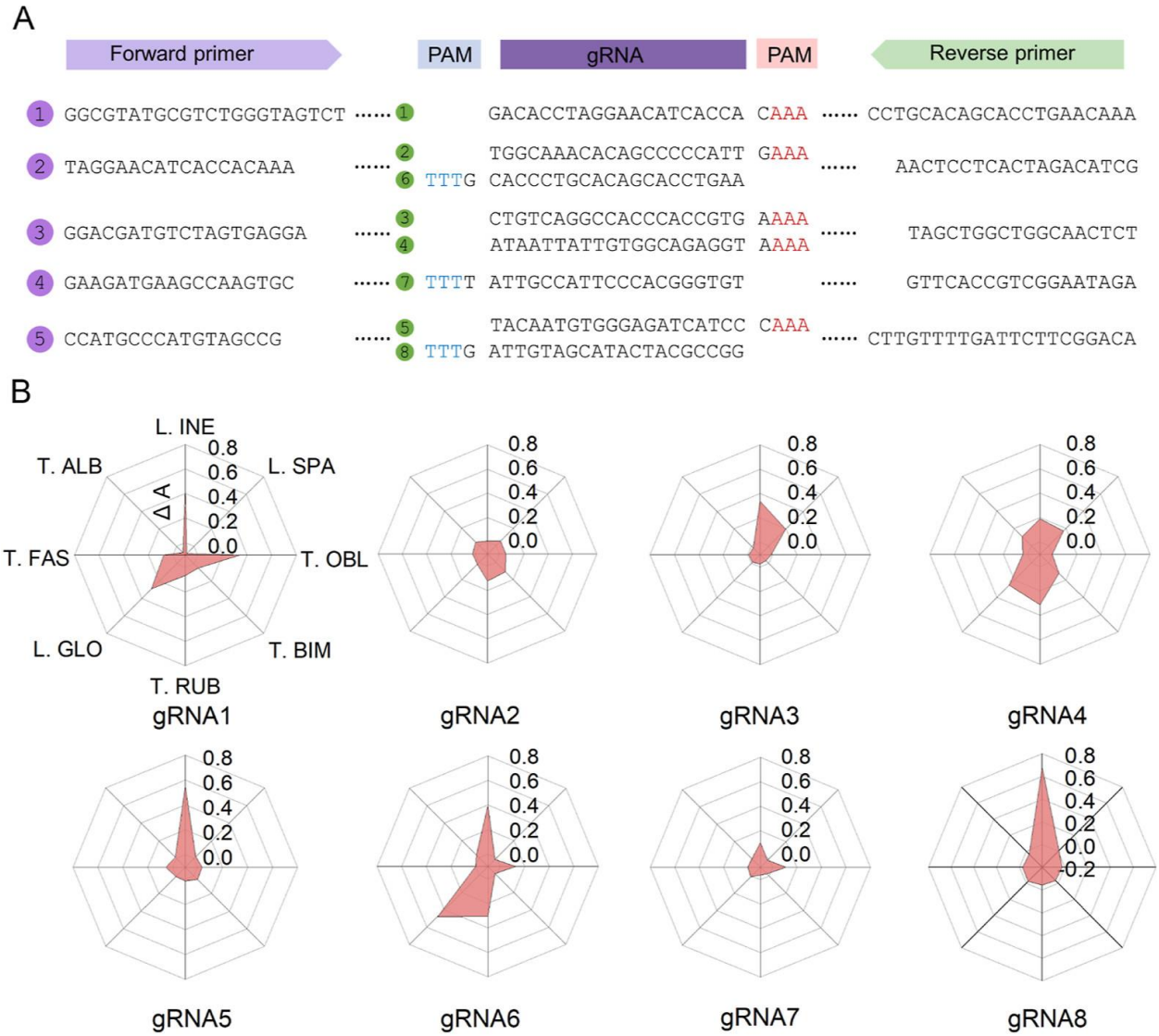

Δ A: The background to signal difference

L. INE: *Lagocephalus inermis* (KT833769.1)

L. SPA: *Lagocephalus spadiceus* (KT833773.1)

T. OBL: *Takifugu oblongus* (KT833777.1)

T. BIM: *Takifugu bimaculatus* (KT833778.1)

T. RUB: *Takifugu rubripes* (KT833774.1)

L. GLO: *Lagocephalus gloveri* (KT833775.1)

T. FAS: *Takifugu fasciatus* (KT833771.1)

T. ALB: *Takifugu alboplumbeus* (KT833780.1)

Optimization of the G-Quadruplex to Serve as the Reporter of Cas12a

We compared several G-quadruplex DNAzymes with different G-rich sequences (Figure 3A, Table S2) in terms of their capability to catalyze the color development of TMB. Results show that all of them had high catalytic activity, and the highest Δ A was presented by G3A6 which was up to 0.52 at

652 nm (Figure 3B). Among these G-quadruplexes, G3A6 yielded the highest oxidation activity toward TMB. When 3 A bases were replaced by 3 T bases, ΔA was decreased from 0.38 (G3A3) to 0.05 (G3T3), and when 6 A bases were replaced by 6 T bases, ΔA was decreased from 0.52 (G3A6) to 0.04 (G3T6) (Figure 3B). The results showed that the activated Cas12a can more effectively cleave poly A than poly T, thus G-quadruplex with A bases in the space between G-rich sequences can serve as a more effective reporter than that with T as space bases. It is reported that Cas12a preferred to cut the ploy-C reporter, followed by the poly-A and poly-T reporters sequentially. (39) The number of A bases in the space of G-rich sequence also affected the efficiency of Cas12a *trans*-cleavage, the values of ΔA of 3 and 6 A bases were 0.38 and 0.52, respectively (Figure 3B). Nevertheless, because the G-C hydrogen bond is very stable, it is not conducive to the formation of the space structure of G-quadruplex and affects its catalytic function. Cas12a *trans*-cleavage of the G-quadruplex has cleavage propensity for base A-rich sequences, and G3A6 could serve as the most efficient reporter of Cas12a based on ΔA. The G-quadruplex DNAzyme reporter eliminates the use of qPCR instruments and the dependence of the time-lengthy electrophoretic process.

Figure 3. Optimization of the sensing conditions. (A) Structure of eight different G-quadruplexes. (B) Absorbance at 652 nm, the ΔA with different G-quadruplexes, and the corresponding visual detection photos (below). (C) Absorbance (652 nm) intensity and the ΔA base on the use of different G-quadruplex concentrations, with the corresponding visual detection photos (below). (D) Absorbance (652 nm) intensity and the ΔA using different PCR cycle numbers. (E) Absorbance at 652 nm and the ΔA with the coloration time of G-quadruplex. Data in A, B, C, and D are mean ± s.d. (n = 3).

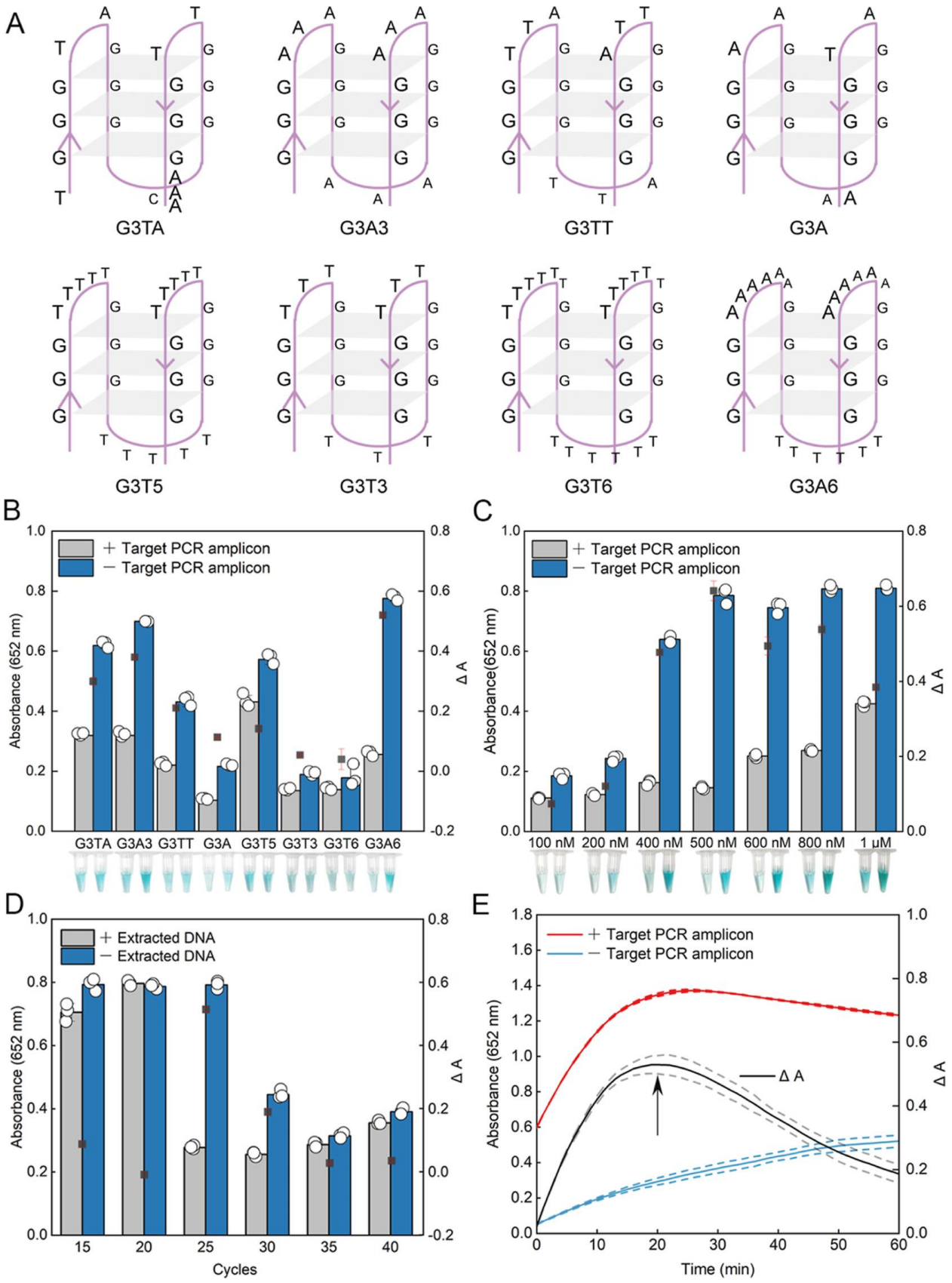
A
G3TA
G3A3
G3TT
G3A
G3T5
G3T3
G3T6
G3A6
B
+ Target PCR amplicon
– Target PCR amplicon
Absorbance (652 nm)
Δ A
G3TA G3A3 G3TT G3A G3T5 G3T3 G3T6 G3A6
C
+ Target PCR amplicon
– Target PCR amplicon
Absorbance(652 nm)
Δ A
100 nM 200 nM 400 nM 500 nM 600 nM 800 nM 1 μM
D
+ Extracted DNA
– Extracted DNA
Absorbance (652 nm)
Δ A
Cycles
E
+ Target PCR amplicon
– Target PCR amplicon
Absorbance (652 nm)
Δ A
Time (min)

Optimization of the Assaying Conditions

The ratio of Cas12a protein-to-G-quadruplex could significantly affect the response of the CRISPR-Cas12a system toward PCR amplicons and thus was optimized. ΔA was the highest of 0.64 at 652 nm when the concentration of G-quadruplex was 500 nM, and the molar ratio of Cas12a protein-to-G-quadruplex was 1:5 (Figure 3B). A further increase of the G-quadruplex reduced ΔA as the background increased. Next, we optimized the coloration time of TMB oxidization via G-quadruplex. When TMB was added for about 20 min, the ΔA at 652 nm was the highest, which was 0.53 (Figure 3D).

We further optimized the procedure of PCR. The cycle numbers could significantly affect the absorbance response of the CRISPR-Cas12a system. PCR with 25 cycles can exhibit a maximum ΔA of 0.51 at 652 nm (Figure 3C). Reducing the cycle number below 25 generated fewer amplicons and thus resulted in a low absorbance change compared to samples without the addition of extracted DNAs. A cycle number over 25 did not significantly contribute to the cleavage of G-quadruplex but dramatically decreased the background absorbance.

Adulteration Performance Test in Meat Mixture

To test the feasibility of the Cricba assay for real-sample analysis under the optimal tested conditions, a series of different proportions (0–100%) of L. inermis to *L. spadiceus* pufferfish meat mixture was prepared. The absorbance decreased with the increased proportion of L. inermis in the pufferfish mixture. A significant difference in absorbance was observed for 0 and 0.1% (w/w) of *L. inermis* contamination levels (Figure 4A) (two-tailed unpaired Student's t-test: *$P < 0.05$), indicating that the Cricba assay could detect as low as 0.1% (w/w) *L. inermis* contamination in the raw meat mixture. The result was further verified using the qPCR method (Figure 4B). Both the Cricba assay and qPCR allowed us to detect the L. inermis component diluted down to 0.1%.

In addition, we compared the sensitivity of the Cricba assay with real-time PCR. We employed serial dilutions of extracted *L. inermis* DNA (0.5 pg/μL, 1 pg/μL, 5 pg/μL, 50 pg/μL, and 5 ng/μL) as

templates. The sensitivity of the Cricba assay was comparable to real-time PCR, and it could detect 0.5 pg/μL target DNA (Figure 4C,D).

Identification of Pufferfish

Although each species of pufferfish has a unique set of morphological characteristics, species identification was difficult for untrained eyes because some of them looked very similar in appearance (Figure 5A). In order to distinguish four common species of pufferfish, including *L. inermis* (GenBank: KT833769), *L. spadiceus* (GenBank: KT833773), *T. bimaculatus* (GenBank: KT833778), and *T. alboplumbeus* (GenBank: KT833780), we designed PCR primers and gRNAs for the above four pufferfish species (Figures S2 and S3, in the Supporting Information). The results showed that the established method could specifically detect the components of four species of pufferfish (Figure 5A,B). For L. spadiceus, the ΔA at 652 nm was 0.660. For *T. bimaculatus*, the ΔA at 652 nm was 0.599, and for *T. alboplumbeus* it was 0.668 (Figure 5B). The corresponding visual detection results were consistent with the absorbance (Figure 5C). The results were consistent with those of real-time PCR (Figure S1, in the Supporting Information), indicating the high specificity of the developed assay. Therefore, the Cricba assay can precisely detect the difference in pufferfish species. The identification of other meat species could be achieved via designing PCR primers and gRNAs target-specific DNA barcodes. Due to the dual recognition induced by PCR primer and gRNAs, the assay could be highly specific for detecting DNA barcodes. Particularly, the colorimetric assay enabled by *trans*-cleavaging the G-quadruplex DNAzyme allows a visual readout of food authenticity by the naked eye.

Figure 4. Quantification performance of the Cricba assay. (A) Typical absorbance curves (500–700 nm) of the Cricba assay corresponding to the addition of different percentages of *L. inermis* added into mixture pufferfish meat (0, 0.1, 1, 5, 10, 20, 40, 60, 80, and 100%). Inner: absorbance at 652 nm for the samples with 0, 0.1, 1, 5 and 10% *L. inermis*, and the corresponding visual detection photos (inside). (B) qPCR amplification curves corresponding to the samples in (A). Inner: the Ct value for the samples with 0, 0.1, 1, 5, and 10% *L. inermis*. (C) Typical absorbance curves (500–700 nm) of the Cricba assay sensitive were tested with 10-fold serial dilutions of extracted *L. inermis* DNA (0.5 pg/μL, 1 pg/μL, 5 pg/μL, 50 μg/μL and 5 ng/μL), and the corresponding visual detection photos (inside). (D) qPCR amplification curves corresponding to samples in (C). Inner: the Ct value and the corresponding visual detection photos for the samples added in the PCR system with 0.5 pg/μL, 1 pg/μL, 5 pg/μL, 50 μg/μL and 5 ng/μL *L. inermis.* Statistical significances were obtained by two-tailed unpaired Student's t-test: *P < 0.05. Data in A, B, C, and D are mean ± s.d. (n = 3).

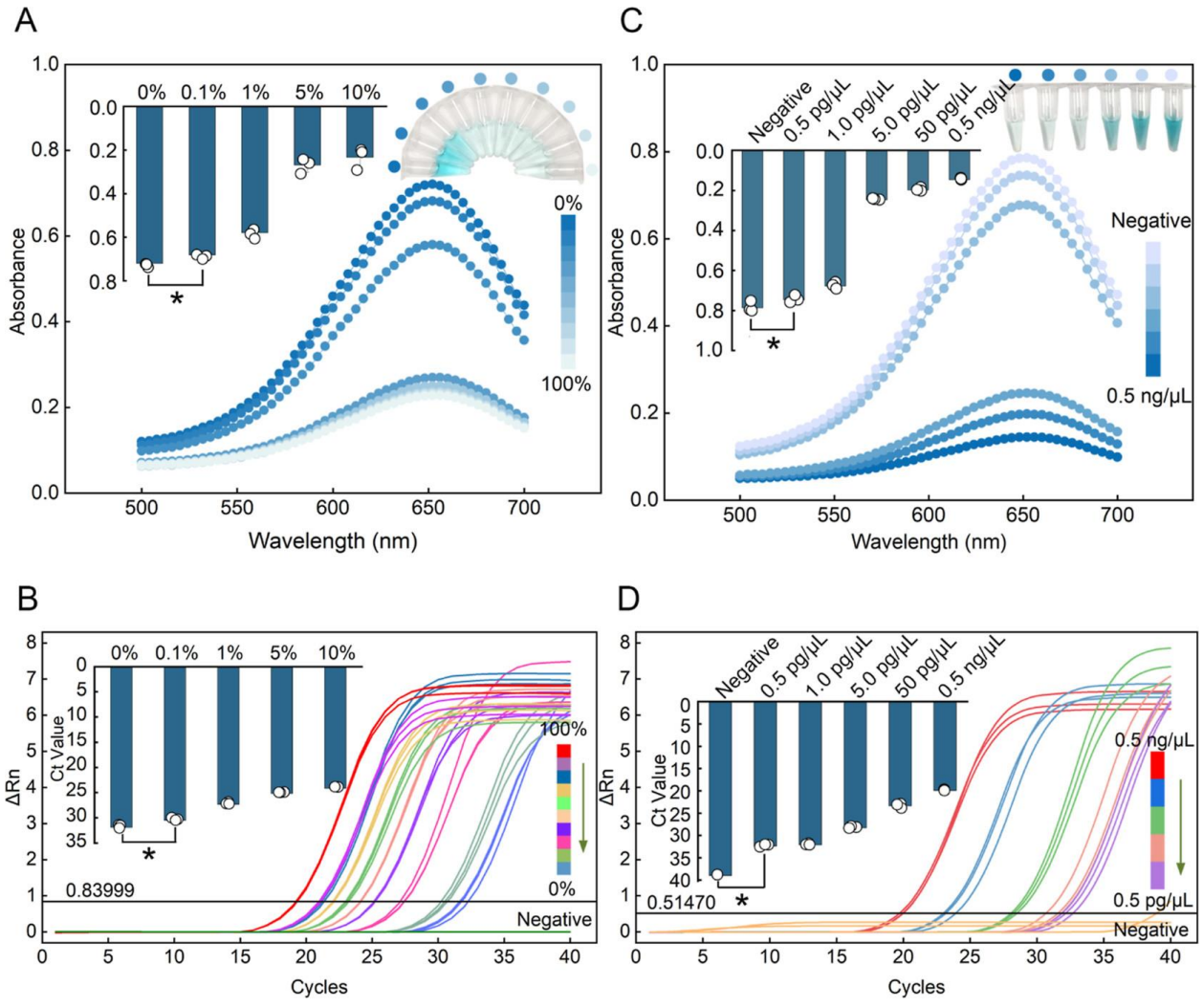

Figure 5. Identification of four species pufferfish (L. SPA, L. INE, T. BIM, and T.ALB) by the Cricba assay. (A) Photos of eight species pufferfish, including *L. inermis* (L. INE), *L. spadiceus* (L. SPA), *T. bimaculatus* (T. BIM), *T. alboplumbeus* (T. ALB), L. gloveri (L. GLO), *T. oblongus* (T. OBL), *T. fasciatus* (T. FAS), and *T. rubripes* (T. RUB). (B) The ΔA at 652 nm after color development by the Cricba assay. (C) The corresponding visual detection results in (B).

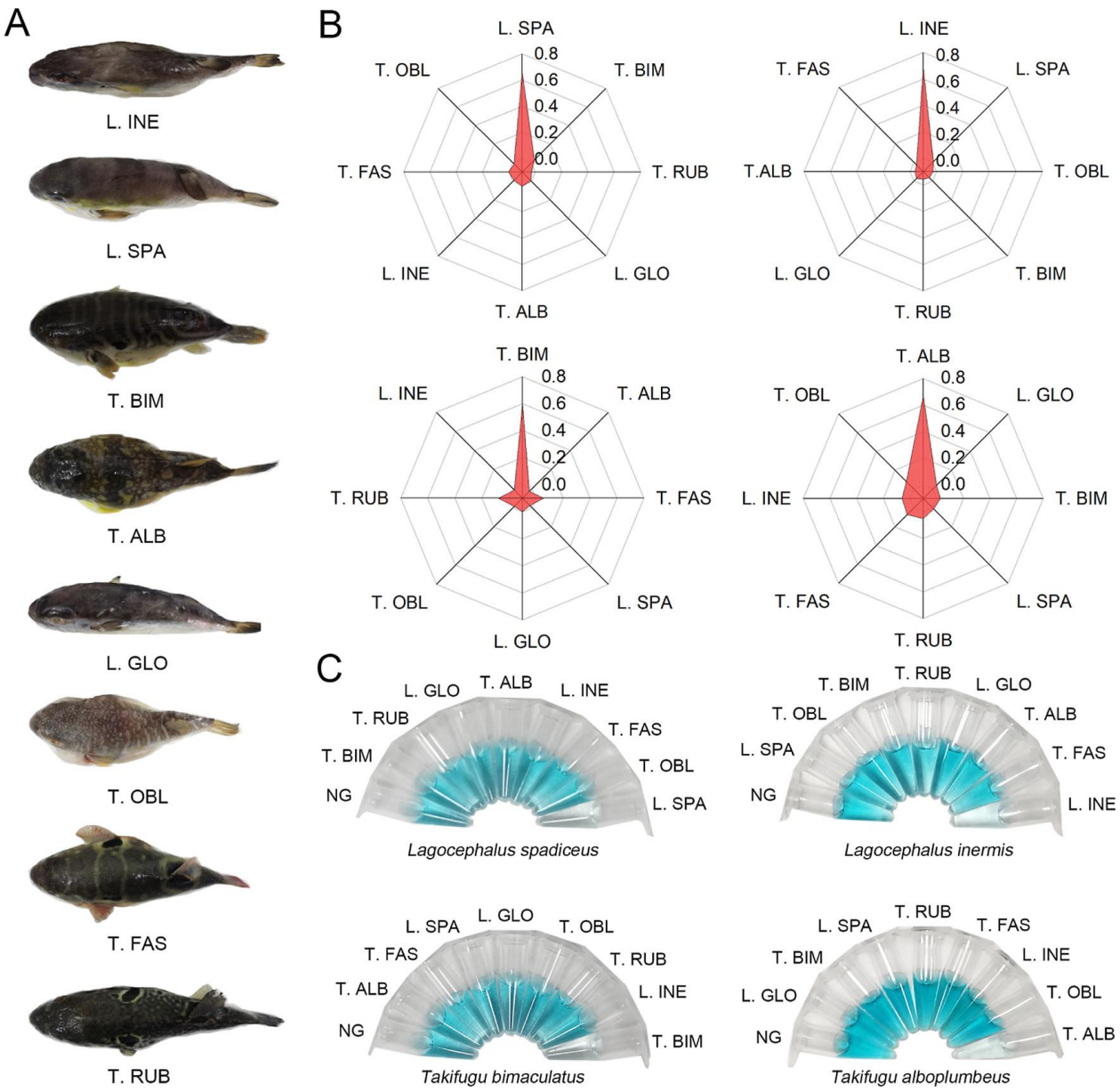

In summary, we developed a colorimetric PCR assay, allowing the visual readout of DNA barcodes and food authenticity by the naked eye. The use of G-quadruplex DNAzyme as the reporter of Cas12a allowed the indication of DNA barcode presence via the color change of TMB, eliminating the

dependence of the expensive qPCR instrument and the time-lengthy electrophoretic process. Dual recognition derived from PCR primers and gRNA excluded the potential non-specific amplification in closely related species, thus guaranteed a high specificity for food authentication. The assay, termed Cricba, could distinguish four species of pufferfish-contaminated samples and permit us to identify the species in complex processed meat samples. Contributing to PCR amplification, Cas12a cleavage reaction, and G-quadruplex oxidation catalysis, the Cricba assay allowed us to detect as low as 0.1% (w/w) pufferfish content. Therefore, the Cricba assay is highly sensitive, highly specific, easily readable, and could be a promising tool for food authenticity.

Acknowledgements

This work was supported by the National Key R&D Program of China (No. 2021YFF0601902), Rejuvenating Liaoning Talents Plan of Liaoning Province (No. XLYC2002106), Open Fund of Key Laboratory of Biotechnology and Bioresources Utilization (Dalian Minzu University), Ministry of Education, China (NO. 0220−118001), and the Researchers Supporting Project Number (No. RSP-2021/138), King Saud University, Riyadh, Saudi Arabia.

References

(1) Visciano, P.; Schirone, M. Food frauds: Global incidents and misleading situations. Trends Food Sci. Technol. 2021, 114, 424−442.

(2) Abbas, O.; Zadravec, M.; Baeten, V.; Mikus, T.; Lesič ́, T.; Vulić, A.; Prpić, J.; Jemersič ́, L.; Pleadin, J. Analytical methods used for the authentication of food of animal origin. Food Chem. 2018, 246, 6−17.

(3) Kappel, K.; Eschbach, E.; Fischer, M.; Fritsche, J. Design of a user-friendly and rapid DNA microarray assay for the authentication of ten important food fish species. Food Chem. 2020, 311, 125884.

(4) Bane, V.; Lehane, M.; Dikshit, M.; O'Riordan, A.; Furey, A.Tetrodotoxin: chemistry, toxicity, source, distribution and detection.Toxins (Basel) 2014, 6, 693−755.

(5) Biessy, L.; Boundy, M. J.; Smith, K. F.; Harwood, D. T.; Hawes, I.; Wood, S. A. Tetrodotoxin in marine bivalves and edible gastropods: A mini-review. Chemosphere 2019, 236, 124404.

(6) Giusti, A.; Ricci, E.; Guarducci, M.; Gasperetti, L.; Davidovich, N.; Guidi, A.; Armani, A. Emerging risks in the European seafood chain: Molecular identification of toxic Lagocephalus spp. in fresh and processed products. Food Control 2018, 91, 311−320.

(7) Bi, H.; Cai, D.; Zhang, R.; Zhu, Y.; Zhang, D.; Qiao, L.; Liu, Y. Mass spectrometry-based metabolomics approach to reveal differ ential compounds in pufferfish soups: Flavor, nutrition, and safety.Food Chem. 2019, 301, 125261.

(8) Zhang, N.; Wang, W.; Li, B.; Liu, Y. Non-volatile taste active compounds and umami evaluation in two aquacultured pufferfish (Takifugu obscurus and Takifugu rubripes). Food Biosci 2019, 32,100468.

(9) Galimberti, A.; De Mattia, F.; Losa, A.; Bruni, I.; Federici, S.; Casiraghi, M.; Martellos, S.; Labra, M. DNA barcoding as a new tool for food traceability. Food Res. Int. 2013, 50, 55−63.

(10) Jiang, X.; Rao, Q.; Mittl, K.; Hsieh, Y.-H. P. Monoclonal antibody-based sandwich ELISA for the detection of mammalian meats. Food Control 2020, 110, 107045.

(11) Mandli, J.; EL Fatimi, I.; Seddaoui, N.; Amine, A. Enzyme immunoassay (ELISA/immunosensor) for a sensitive detection of pork adulteration in meat. Food Chem. 2018, 255, 380−389.

(12) Grundy, H. H.; Brown, L.; Romero, M.; Donarski, J. Review: Methods to determine offal adulteration in meat products to support enforcement and food security. Food Chem. 2023, 399, 133818.

(13) Wu, Y.; Liu, J.; Li, H.-t.; Zhang, T.; Dong, Y.; Deng, S.; Lv, Y.; He, Q.; Deng, R. CRISPR-Cas system meets DNA barcoding: Development of a universal nucleic acid test for food authentication. Sens. Actuators B-Chem. 2022, 353, 131138.

(14) Galimberti, A.; Casiraghi, M.; Bruni, I.; Guzzetti, L.; Cortis, P.; Berterame, N. M.; Labra, M. From DNA barcoding to personalized nutrition: the evolution of food traceability. Curr. Opin. Food Sci. 2019, 28, 41−48.

(15) Carvalho, D. C.; Palhares, R. M.; Drummond, M. G.; Frigo, T. B. DNA Barcoding identification of commercialized seafood in South Brazil: A governmental regulatory forensic program. Food Control 2015, 50, 784−788.

(16) Trivedi, S.; Aloufi, A. A.; Ansari, A. A.; Ghosh, S. K. Role of DNA barcoding in marine biodiversity assessment and conservation: An update. Saudi J. Biol. Sci. 2016, 23, 161−171.

(17) Nagalakshmi, K.; Annam, P.-K.; Venkateshwarlu, G.; Pathakota, G.-B.; Lakra, W. S. Mislabeling in Indian seafood: An investigation using DNA barcoding. Food Control 2016, 59, 196−200.

(18) Sultana, S.; Ali, M. E.; Hossain, M. A. M.; Asing; Naquiah, N.; Zaidul, I. S. M. Universal mini COI barcode for the identification of fish species in processed products. Food Res. Int. 2018, 105, 19−28.

(19) Santaclara, F. J.; Velasco, A.; Pérez-Martín, R. I.; Quinteiro, J.; Rey-Méndez, M.; Pardo, M. A.; Jimenez, E.; Sotelo, C. G. Development of a multiplex PCR-ELISA method for the genetic

authentication of Thunnus species and Katsuwonus pelamis in food products. Food Chem. 2015, 180, 9−16.

(20) Ramos-Gómez, S.; Busto, M. D.; Albillos, S. M.; Ortega, N. Novel qPCR systems for olive (Olea europaea L.) authentication in oils and food. Food Chem. 2016, 194, 447−454.

(21) Yu, W.; Chen, Y.; Wang, Z.; Qiao, L.; Xie, R.; Zhang, J.; Bian, S.; Li, H.; Zhang, Y.; Chen, A. Multiple authentications of high-value milk by centrifugal microfluidic chip-based real-time fluorescent LAMP. Food Chem. 2021, 351, 129348.

(22) Wang, Z.; Li, T.; Yu, W.; Qiao, L.; Yang, S.; Chen, A. A low cost novel lateral flow nucleic acid assay (LFNAA) for yak milk authentication. Lwt 2020, 122, 109038.

(23) Khaksar, R.; Carlson, T.; Schaffner, D. W.; Ghorashi, M.; Best, D.; Jandhyala, S.; Traverso, J.; Amini, S. Unmasking seafood mislabeling in U.S. markets: DNA barcoding as a unique technology for food authentication and quality control. Food Control 2015, 56,

71−76.

(24) Schelm, S.; Siemt, M.; Pfeiffer, J.; Lang, C.; Tichy, H. V.; Fischer, M. Food Authentication: Identification and Quantitation of Different Tuber Species via Capillary Gel Electrophoresis and Real Time PCR. Foods 2020, 9(). DOI: 10.3390/foods9040501

(25) Lo, Y. T.; Shaw, P. C. DNA-based techniques for authentication of processed food and food supplements. Food Chem. 2018, 240,

767−774.

(26) Sampson, T. R.; Weiss, D. S. CRISPR-Cas systems: new players in gene regulation and bacterial physiology. Front Cell Infect Mi 2014,

4, 37.

(27) Li, S. Y.; Cheng, Q. X.; Liu, J. K.; Nie, X. Q.; Zhao, G. P.; Wang, J. CRISPR-Cas12a has both cis- and *trans*-cleavage activities on single-stranded DNA. Cell Res 2018, 28, 491−493.

(28) Li, S. Y.; Cheng, Q. X.; Wang, J. M.; Li, X. Y.; Zhang, Z. L.; Gao, S.; Cao, R. B.; Zhao, G. P.; Wang, J. CRISPR-Cas12a-assisted nucleic acid detection. Cell Discov 2018, 4, 20.

(29) Swarts, D. C.; Jinek, M. Mechanistic Insights into the cis- and trans-Acting DNase Activities of Cas12a. Mol. Cell 2019, 73, 589−600e4.

(30) Tao, D.; Liu, J.; Li, Q.; Jiang, Y.; Xu, B.; Khazalwa, E. M.; Gong, P.; Xu, J.; Ma, Y.; Ruan, J.; Niu, L.; Xie, S. A Simple, Affordable, and Rapid Visual CRISPR-Based Field Test for Sex Determination of Earlier Porcine Embryos and Pork Products. Mol. Biotechnol. 2022,

15, 1−10.

(31) Wang, Y.; Zhang, Y.; Chen, J.; Wang, M.; Zhang, T.; Luo, W.; Li, Y.; Wu, Y.; Zeng, B.; Zhang, K.; Deng, R.; Li, W. Detection of SARS-CoV-2 and Its Mutated Variants via CRISPR-Cas13-Based Transcription Amplification. Anal. Chem. 2021, 93, 3393−3402.

(32) Broughton, J. P.; Deng, X.; Yu, G.; Fasching, C. L.; Servellita, V.; Singh, J.; Miao, X.; Streithorst, J. A.; Granados, A.; Sotomayor Gonzalez, A.; Zorn, K.; Gopez, A.; Hsu, E.; Gu, W.; Miller, S.; Pan, C.Y.; Guevara, H.; Wadford, D. A.; Chen, J. S.; Chiu, C. Y. CRISPR Cas12-based detection of SARS-CoV-2. Nat. Biotechnol. 2020, 38,870−874.

(33) Yang, B.; Shi, Z.; Ma, Y.; Wang, L.; Cao, L.; Luo, J.; Wan, Y.;Song, R.; Yan, Y.; Yuan, K.; Tian, H.; Zheng, H. LAMP assay coupled with CRISPR/Cas12a system for portable detection of African swine fever virus. Transbound. Emerg. Dis. 2022, 69, e216−e223.

(34) Zhang, M.; Liu, C.; Shi, Y.; Wu, J.; Wu, J.; Chen, H. Selective endpoint visualized detection of Vibrio parahaemolyticus with CRISPR/Cas12a assisted PCR using thermal cycler for on-site application. Talanta 2020, 214, 120818.

(35) Yang, H.; Chen, J.; Yang, S.; Zhang, T.; Xia, X.; Zhang, K.;Deng, S.; He, G.; Gao, H.; He, Q.; Deng, R. CRISPR/Cas14a-Based Isothermal Amplification for Profiling Plant MicroRNAs. Anal. Chem. 2021, 93, 12602−12608.

(36) Aquino-Jarquin, G. Recent progress on rapid SARS-CoV-2/ COVID-19 detection by CRISPR-Cas13-based platforms. Drug Discov. Today 2021, 26, 2025−2035.

(37) Wu, L.; Zhou, T.; Huang, R. A universal CRISPR/Cas9-based electrochemiluminescence probe for sensitive and single-base-specific DNA detection. Sens. Actuators B-Chem. 2022, 357, 131411.

(38) Zhu, Z.; Li, R.; Zhang, H.; Wang, J.; Lu, Y.; Zhang, D.; Yang, L. PAM-free loop-mediated isothermal amplification coupled with CRISPR/Cas12a cleavage (Cas-PfLAMP) for rapid detection of rice pathogens. Biosens. Bioelectron. 2022, 204, 114076.

(39) You, Y.; Zhang, P.; Wu, G.; Tan, Y.; Zhao, Y.; Cao, S.; Song, Y.; Yang, R.; Du, Z. Highly Specific and Sensitive Detection of Yersinia pestis by Portable Cas12a-UPTLFA Platform. Front Microbiol 2021, 12, 700016. Journal of Agricultural and Food Chemistry pubs.acs.org/JAFC Article https://doi.org/10.1021/acs.jafc.2c05974 J. Agric. Food Chem. 2022, 70, 14052−14060

Supporting Information

CRISPR-based Colorimetric Nucleic Acid Tests for Visual Readout of DNA Barcode for Food Authenticity

Xinying Yin[1], Hao Yang[2], Yongzhe Piao[1], Yulin Zhu[2], Qiuyue Zheng[1], Mohammad Rizwan Khan[3], Yong Zhang[2], Rosa Busquets[4], Bing Hu[1], Ruijie Deng[2,*], Jijuan Cao[1,*]

[1] Key Laboratory of Biotechnology and Bioresources Utilization of Ministry of Education, Dalian Minzu University, Dalian 116600, China

[2] College of Biomass Science and Engineering, Healthy Food Evaluation Research Center, Sichuan University, Chengdu 610065, China

[3] Department of Chemistry, College of Science, King Saud University, Riyadh, 11451, Saudi Arabia

[4] School of Life Sciences, Pharmacy and Chemistry, Kingston University, Penrhyn Road, KT1 2EE, Kingston Upon Thames, United Kingdom

* Corresponding authors: drj17@scu.edu.cn; caojijuan@dlnu.edu.cn

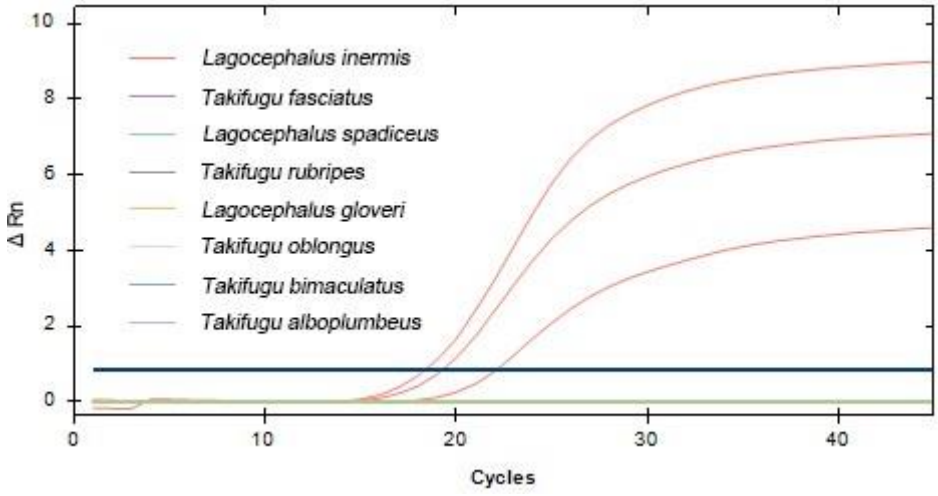

Figure S1. Specificity test for detecting *Lagocephalus inermis* using real-time quantitative PCR detection. The average Ct value of *Lagocephalus inermis* was 19.83±1.95 and other seven species pufferfish were undetected.

A *Lagocephalus inermis* cytochrome oxidase subunit I (COI) gene, GenBank: KT833769.1

GGCGTATGCGTCTGGGTAGTCTGAGTATCGACGAGGCATTCCGGCCAGTCCCAGGAAGTGTTGTG
GGAAGAAGGTTAGGTTGACACCTAGGAACATCACCACAAAGTGGATTTTTGTTCAGGTGCTGTGC
AGGGTGTATCCCGAGAAAAGGGGGAATCAATGTACGAAGGCTCCCATGATGGCAAACACAGCCCC
CATTGAAAGGACGTAGTGGAAGTGGGCTACTACGTAGTATGTGTCATGGAGGACGATGTCTAGTG
AGGAGTTGGCTAGGACGATTCCTGTCAGGCCACCCACCGTGAAAAGGAAGATGAAGCCAAGTGCT
CAGAGCATTGGGGTCTCTCACTTAATTGAGCCCCCGTGCAGAGTTGCCAGCCAGCTAAACACTTT
TACACCCGTGGGAATGGCAATAATTATTGTGGCAGAGGTAAAATAGGCTCGAGTGTCCACGTCTA
TTCCGACGGTGAACATGTGATGGGCTCAGACAATGAAGCCCAGAAGGCCAATAGCCATTATTGCC
CACACCATGCCCATGTAGCCGAAGGGTTCTTTTTTGCCGGCGTAGTATGCTACAATGTGGGAGAT
CATCCCAAAGCCAGGGAGAATGAGAATGTAGACTTCAGGGTGTCCGAAGAATCAAAACAAGTGTT
GATAGAGGATTGGATCTCCTCCTCCTGCAGG

B *Lagocephalus spadiceus* cytochrome oxidase subunit I (COI) gene, GenBank: KT833773.1

GGCGTATGCGTCTGGGTAGTCTGAGTATCGACGAGGTATTCCGGCCAGGCCTAGGAAGTGTTG
GGGGAAGAAGGTTAGATTTTACACCCAGGAACATTACCATAAAATGGATTTTTGTCCAGGTGCT
GTGCAGGGTGTAACCTGAGAAGAGCGGGAATCAGTGAACGAAAGCCCCTATGATGGCAAATAC
AGCACCCATCGAGAGGACATAGTGGAAGTGGGCAGCTACATAATATGTGTCATGAAGGACGAT
GTCTAGGGACGAGTTGGCTAGGACAATTCCTGTCAGGCCCCCCACCGTAAAGAGGAAAATAAA
TCCGAGTGCCCAAAGCATTGGGGTCTCTCACTTAATTGAGCCCCCGTGGAGGGTGGCTAATCA
GCTAAATACTTTGACCCCTGTTGGAATGGCAATGATCATGGTGGCGGATGTGAAGTAGGCCCG
GGTGTCTACGTCTATACCAACAGTGAACATGTGATGGGCTCAGACAATGAAGCCTAGAAGACC
GATGGCCATTATTGCCCAGACCATGCCCATATAACCAAAAGGCTCCTTTTTGCCGGCGTAGTA
GGCTACGATGTGTGAAATCATTCCGAAGCCGGGGAGAATAAGAATATAGACCTCGGGGTGGCC
AAAGAATCAGAACAGGTGTTGGTAGAGGATCGGATCTCCTCCTCCTGCAGG

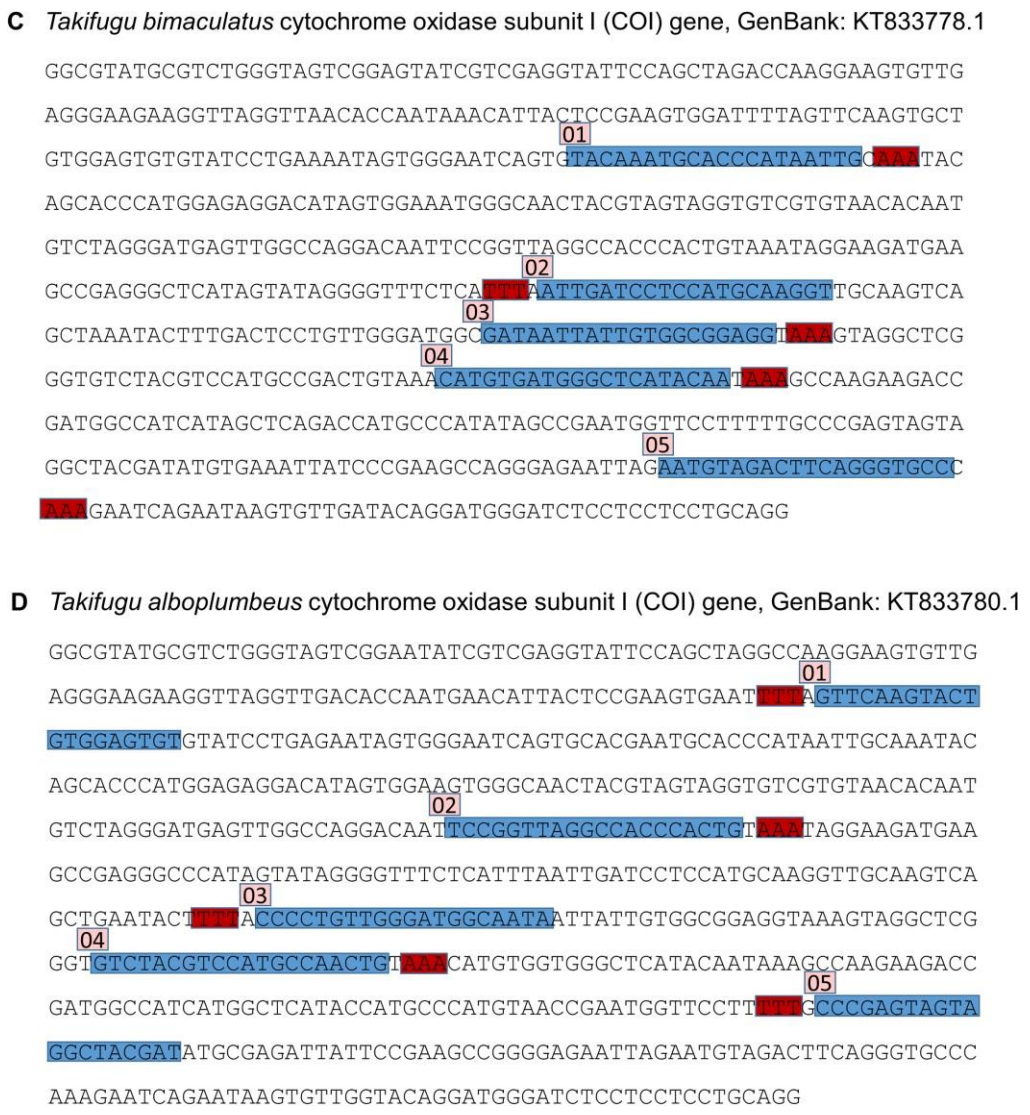

Figure S2. COI gene sequence of *Lagocephalus inermis* (A), *Lagocephalus spadiceus* (B), *Takifugu bimaculatus* (C) and *Takifugu alboplumbeus* (D). Target DNAs were highlighted in blue and named in pink. The PAMs of target DNA fragments were marked in red.

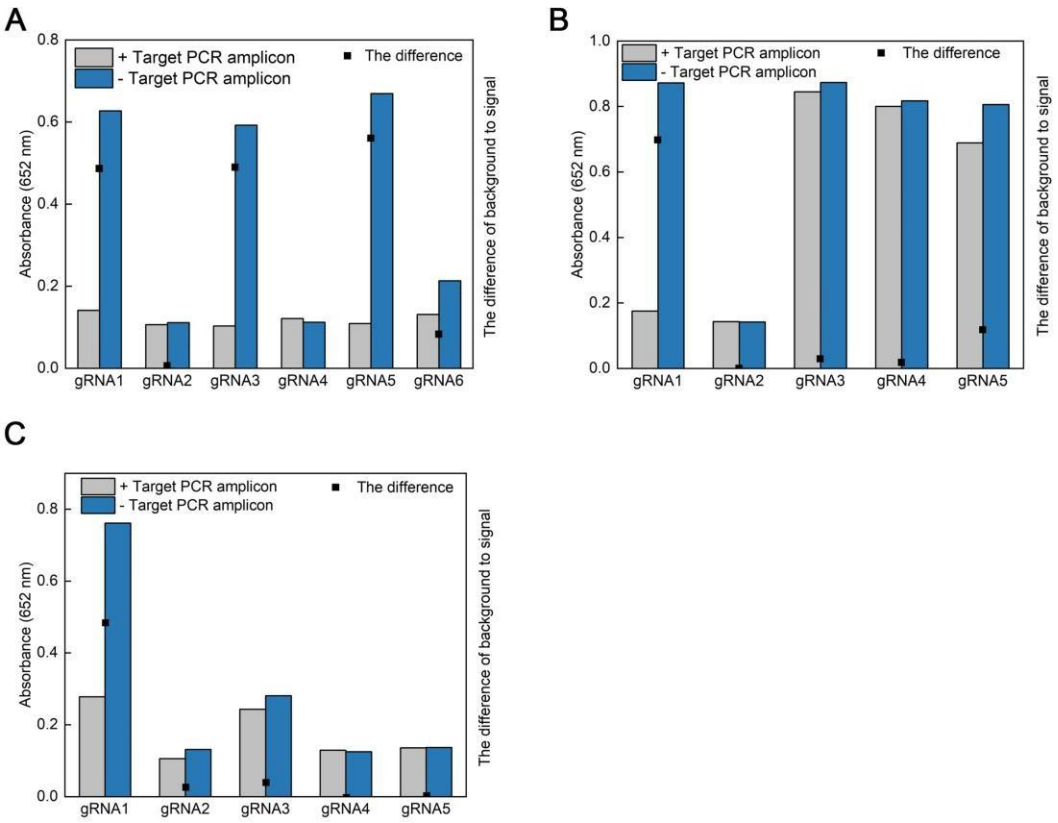

Figure S3. gRNA screening for *Lagocephalus spadiceus* (A), *Takifugu bimaculatus* (B) and *Takifugu alboplumbeus* (C).

Table S1. DNA oligonucleotide sequences

	Oligonucleotide name	Region (nt)	Sequence (5'-3')
01	L.INE-Cas-1	82-101	GACACCTAGGAACATCACCAATCTACACTTAGTAGAAATTACTATAGTGAGTCGTATTA
02	L. INE-Cas-2	180-199	TGGCAAACACAGCCCCCATTATCTACACTTAGTAGAAATTACTATAGTGAGTCGTATTA
03	L. INE-Cas-3	282-301	CTGTCAGGCCACCCACCGTGATCTACACTTAGTAGAAATTACTATAGTGAGTCGTATTA
04	L. INE-Cas-4	410-429	ATAATTATTGTGGCAGAGGTATCTACACTTAGTAGAAATTACTATAGTGAGTCGTATTA
05	L. INE-Cas-5	571-590	TACAATGTGGGAGATCATCCATCTACACTTAGTAGAAATTACTATAGTGAGTCGTATTA
06	L. INE-Cas-6	117-136	CACCCTGCACAGCACCTGAAATCTACACTTAGTAGAAATTACTATAGTGAGTCGTATTA
07	L. INE-Cas-7	392-411	ATTGCCATTCCCACGGGTGTATCTACACTTAGTAGAAATTACTATAGTGAGTCGTATTA
08	L. INE-Cas-8	557-576	ATTGTAGCATACTACGCCGGATCTACACTTAGTAGAAATTACTATAGTGAGTCGTATTA
09	L. SPA-Cas-1	84-103	TATGGTAATGTTCCTGGGTGATCTACACTTAGTAGAAATTACTATAGTGAGTCGTATTA
10	L. SPA-Cas-2	117-136	CACCCTGCACAGCACCTGGAATCTACACTTAGTAGAAATTACTATAGTGAGTCGTATTA
11	L. SPA-Cas-3	146-165	AAGAGCGGGAATCAGTGAACATCTACACTTAGTAGAAATTACTATAGTGAGTCGTATTA
12	L. SPA-Cas-4	361-380	GTGGAGGGTGGCTAATCAGCATCTACACTTAGTAGAAATTACTATAGTGAGTCGTATTA
13	L. SPA-Cas-5	520-539	CCAGACCATGCCCATATAACATCTACACTTAGTAGAAATTACTATAGTGAGTCGTATTA
14	L. SPA-Cas-6	557-576	ATCGTAGCCTACTACGCCGGATCTACACTTAGTAGAAATTACTATAGTGAGTCGTATTA
15	T. BIM-Cas-1	163-182	TACAAATGCACCCATAATTGATCTACACTTAGTAGAAATTACTATAGTGAGTCGTATTA
16	T. BIM-Cas-2	350-369	ACCTTGCATGGAGGATCAATATCTACACTTAGTAGAAATTACTATAGTGAGTCGTATTA
17	T. BIM-Cas-3	409-428	GATAATTATTGTGGCGGAGGATCTACACTTAGTAGAAATTACTATAGTGAGTCGTATTA
18	T. BIM-Cas-4	468-487	CATGTGATGGGCTCATACAAATCTACACTTAGTAGAAATTACTATAGTGAGTCGTATTA
19	T. BIM-Cas-5	610-629	AATGTAGACTTCAGGGTGCCATCTACACTTAGTAGAAATTACTATAGTGAGTCGTATTA
20	T. ALB-Cas-1	116-135	ACACTCCACAGTACTTGAACATCTACACTTAGTAGAAATTACTATAGTGAGTCGTATTA
21	T. ALB-Cas-2	280-299	TCCGGTTAGGCCACCCACTGATCTACACTTAGTAGAAATTACTATAGTGAGTCGTATTA
22	T. ALB-Cas-3	393-412	TATTGCCATCCCAACAGGGGATCTACACTTAGTAGAAATTACTATAGTGAGTCGTATTA

23	T. ALB-Cas-4	445-464	GTCTACGTCCATGCCAACTGATCTACACTTAGTAGAAATTACTATAGTGAGTCGTATTA
24	T. ALB-Cas-5	557-576	ATCGTAGCCTACTACTCGGGATCTACACTTAGTAGAAATTACTATAGTGAGTCGTATTA
25	L. INE-F-1	525-542	CCATGCCCATGTAGCCG
26	L. INE-R-1	647-626	CTTGTTTTGATTCTTCGGACA
27	L. INE-F-2	1-22	GGCGTATGCGTCTGGGTAGTCT
28	L. INE-R-2	133-114	CCTGCACAGCACCTGAACAAA
29	L. INE-F-3	88-101	TAGGAACATCACCACAAA
30	L. INE-R-3	267-249	AACTCCTCACTAGACATCG
31	L. INE-F-4	246-265	GGACGATGTCTAGTGAGGA
32	L. INE-R-4	382-365	TAGCTGGCTGGCAACTCT
33	L. INE-F-5	307-325	GAAGATGAAGCCAAGTGC
34	L. INE-R-5	469-452	GTTCACCGTCGGAATAGA
35	L. SPA-F-1	7-22	TGCGTCTGGGTAGTCTGAGT
36	L. SPA-R-1	162-145	CACTGATTCCCGCTCTTC
37	L. SPA-F-2	244-263	ACACCCAGGAACATTACC
38	L. SPA-R-2	384-367	CCAACTCGTCCCTAGACAT
39	L. SPA-F-3	308-325	AAAATAAATCCGAGTGCC
40	L. SPA-R-3	436-419	CTACTTCACATCCGCCAC
41	L. SPA-F-4	473-491	TGATGGGCTCAGACAATG
42	L. SPA-R-4	596-579	GCTTCGGAATGATTTCAC
43	T. BIM-F-1	27-44	ATCGTCGAGGTATTCCAG
44	T. BIM-R-1	223-206	TGCCCATTTCCACTATGT
45	T. BIM-F-2	274-291	GACAATTCCGGTTAGGC
46	T. BIM-R-2	405-387	ATCCCAACAGGAGTCAAAG

47	T. BIM-F-3	381-401	TAAATACTTTGACTCCTGTT
48	T. BIM-R-3	528-512	ATGGTCTGAGCTATGATG
49	T. BIM-F-4	486-505	CAATAAAGCCAAGAAGACC
50	T. BIM-R-4	665-648	ATCCCATCCTGTATCAAC
51	T. ALB-F-1	27-44	ATCGTCGAGGTATTCCAG
52	T. ALB-R-1	223-206	TGCCCACTTCCACTATGT
53	T. ALB-F-2	202-221	GAGGACATAGTGGAAGTGG
54	T. ALB-R-2	399-381	CAGGGGTAAAAGTATTCA
55	T. ALB-F-3	329-348	AGTATAGGGGTTTCTCATT
56	T. ALB-R-3	502-484	TCTTCTTGGCTTTATTGTA
57	T. ALB-F-4	486-505	CAATAAAGCCAAGAAGACC
58	T. ALB-R-4	665-648	ATCCCATCCTGTACCAAC
59	Promoter		TAATACGACTCACTATAGGG
60	Synthetic Target sequence		ATTGTAGCATACTACGCCGG

Table S2. G-quadurplex sequences

	G-quadurplex name	Sequence (5'-3')
01	G3-TA	TGGGTAGGGCGGGTTGGGAAA
02	G3A3	GGGAAAGGGAAAGGGAAAGGG
03	G3-TT	GGGTTAGGGTTAGGGTTAGGG
04	G3-A	GGGAAGGGAGGGATGGGA
05	G3T5	GGGTTTTTGGTTTTTGGTTTTTGGG
06	G3T3	GGGTTTGGGTTTGGGTTTGGG
07	G3T6	GGGTTTTTTGGGTTTTTTGGGTTTTTTGGG
08	G3A6	GGGAAAAAAGGGAAAAAAGGGAAAAAAGGG